Mesophase Behavior in Thermotropic Polyethers Based on the Semiflexible Mesogen 1-(4-Hydroxyphenyl)-2-(2-methyl-4-hydroxyphenyl)ethane

Michael A. Yandrasits, Stephen Z. D. Cheng,* and Anqiu Zhang

Institute and Department of Polymer Science, College of Polymer Science and Polymer Engineering, University of Akron, Akron, Ohio 44325-3909

Jinlong Cheng and Bernhard Wunderlich

Department of Chemistry, University of Tennessee, Knoxville, Tennessee 37996-1600

Virgil Percec

Department of Macromolecular Science, Case Western Reserve University, Cleveland, Ohio 44106-2699

Received August 12, 1991; Revised Manuscript Received December 26, 1991

ABSTRACT: A series of thermotropic polyethers consisting of a semiflexible mesogen [1-(4-hydroxyphenyl)-2-(2-methyl-4-hydroxyphenyl)ethane] with methylene flexible spacers (n = 4–12) (MBPE-n) has been characterized through thermal analysis, wide-angle X-ray diffraction, small-angle X-ray scattering, polarized light microscopy, and solid-state nuclear magnetic resonance. A mesophase is observed for MBPE-n=odd polyethers on cooling from the isotropic melt and found to be monotropic. Crystallization will follow either on further cooling or on isothermal annealing. MBPE-n=even polyethers exhibit rapid crystallization during cooling, with little cooling-rate dependence. Contributions to the enthalpy and the entropy of mesophase transition from both the semiflexible mesogen and methylene units can be determined. The polymers with n = odd show that the flexible spacers mainly contribute to the thermal transition properties. One can thus conclude that the mesophase in these polyethers results from the coupled action of the methylene units with the semiflexible mesogen. The primary contribution to the order in the mesophase, however, is due to the methylenes.

Introduction

One major class of liquid-crystalline polymers is the thermotropic, main-chain mesogen–nonmesogen type.[1-15] The polymer repeating units consist of a rigid mesogenic group, usually aromatic or cyclic hydrocarbons, and a flexible spacer, usually a series of methylene, ethylene oxide, or other flexible linkages. The generally accepted mechanism of liquid-crystal formation in the polymers entails the preferential alignment of the mesogenic groups, analogous to small-molecule liquid crystals. Based on their phase behavior, two subclasses of these liquid-crystal polymers can be identified. One is enantiotropic, where the polymer exhibits a liquid-crystal phase both on heating and cooling. The other is monotropic, where the liquid-crystal phase can be observed only on cooling with the condition that the sample is supercooled to bypass the crystallization process.

The orientation in liquid-crystal polymers is principally associated with both mesogenic groups and flexible spacers.[16-19] The contribution to the orientational order in the liquid-crystal phase by mesogenic groups is critically dependent upon dipolar effects, polarity, rigidity, and geometrical factors of the mesogen. On the other hand, contributions from the flexible spacers depend on the chemical structure, such as methylene or ethylene oxide linkages, and, in the methylene case, on the parity (odd or even) of the flexible spacers. This odd–even effect manifests itself in a drastic alternation in the temperature of isotropization (T_i), as well as the enthalpy and the entropy of transition (ΔH_i and ΔS_i). For most cases the polymers with an even number of methylene units exhibit a higher degree of orientation than polymers with an odd number.[9]

Quantitative determination of the contributions from the mesogenic group and the flexible spacer has been achieved for specific polymers only. General rules of such determinations are still awaited. Nevertheless, it is known that when the enthalpy or the entropy of transition is plotted versus the number of units in a flexible spacer, the intercepts and the slopes of these linear lines are the respective coupled contributions of mesogen order and spacer order changes at the liquid-crystal transition. This technique was first reported by Blumstein and Blumstein on one series of (4,4′-dihydroxy-2,2′-dimethylazoxybenzene)alkanedioic acid (ME9-Sn) polymers. Their data are reprinted as follows with their chemical structures:[6,19]

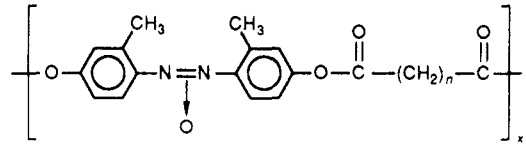

n = 2–14

	ΔH_i, kJ/mol	ΔS_i, J/(K mol)
even		
mesogen	4.7	7.55
methylene	0.16	0.87
odd		
mesogen	0.94	1.41
methylene	0.19	0.57

In addition, a series of liquid-crystal poly(ester amides) with different numbers of methylene spacers were synthesized by Aharoni et al.[20] He showed through wide-angle X-ray diffraction results and solid-state ^{13}C nuclear

* To whom all correspondence should be addressed.

0024-9297/92/2225-2112$03.00/0

Table I
MBPE-n GPC Data[a]

MBPE-n	M_n	M_w/M_n	MBPE-n	M_n	M_w/M_n
4	4 100	1.89	9	20 600	1.38
5	19 000	1.90	10	14 100	2.27
6	14 100	2.42	11	28 500	2.02
7	22 100	2.76	12	29 900	2.62
8	10 400	1.87			

[a] Percec, V.; Yourd, R. *Macromolecules* 1989, 22, 524.

magnetic resonance spectroscopy that the methylenes between the amide groups exist exclusively in the all-trans conformation in the liquid-crystal phase. An attempt has also been made by Percec and Tsuda to understand the contributions of a mesogenic group and flexible spacer with similar extrapolation.[21]

On the other hand, polymers with ethylene oxide linkages do not exhibit an odd–even effect and the orientation is generally due to the mesogenic group only. An example is one series of poly(azomethine ether)s with different numbers of ethylene oxide linkages. With an increase in the number of flexible spacer units, the enthalpy and the entropy of transition are almost constant; ΔH_i is about 2 kJ/mol, and ΔS_i is about 3 J/(K mol).[15] The spacer thus acts as a "diluent" in these polymer liquid crystals. The question arises whether there is a case where the orientation in the liquid-crystal phase is mainly attributed to the orientation of the flexible spacer.

The polymers in this study are a series of polyethers where the mesogenic group consists of two phenylene units connected by a flexible ethylene unit. The flexible spacers are methylene units varying from 4 to 12 and are connected to the mesogen by an ether linkage. The polymer structure is

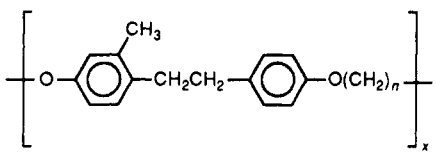

n = 4–12

and has been designated MBPE-n, where n is the number of methylene units in the flexible spacer. A monotropic mesophase has been identified in this series of polyethers with n = odd. The systematic study of the thermodynamic transition properties (T_i, ΔH_i, and ΔS_i), structure, morphology, and molecular motion changes leads to the discussion on the origin of the orientation in the mesophase of these polymers.

Experimental Section

Materials. The synthesis of MBPE polyethers involves coupling 1-(4-hydroxyphenyl)-2-(2-methyl-4-hydroxyphenyl)-ethane and α,ω-dibromoalkanes and has been published elsewhere.[22,23] The polymers used in this study were characterized by gel permeation chromatography (GPC). The number-average molecular mass, $\bar{M}_n$, and polydispersity are listed in Table I. The values for $\bar{M}_n$ are determined with polystyrene as the standard; they should thus be used only for internal comparison between MBPE homologues and not as absolute molecular weight values.

Differential Scanning Calorimetry (DSC). Thermal measurements were performed on a Perkin-Elmer DSC-2 and a Seiko DSC 210. The DSCs were calibrated with an indium standard at all heating and cooling rates used (0.31–80 K/min). All samples were run under a dry-nitrogen atmosphere. Typical sample weights were 6–12 mg when the heating and cooling rates were slow (10 K/min or slower). With increasing the rates, the sample weights were decreased correspondingly. For example, at a rate of 80 K/min, the sample weights for these polymers were only about 0.1 mg.

Samples were heated to about 20 K above the melting temperature and held for 2 min prior to each experiment. Nonisothermal experiments entailed cooling the sample from 20 K above its melt temperature to 230 K at various rates. Isothermal experiments were conducted by quenching the molten sample to the preset temperature in the DSCs and recording the heat flow on a time basis. These samples were then immediately heated at 10 K/min to above the melt temperature.

Sequential cooling and heating experiments were also conducted. The samples were cooled at 10 K/min to the temperature which is slightly below the first transition peak and isothermally held there for present times. The samples were then reheated at 10 K/min.

Wide-Angle X-ray Diffraction (WAXD). A Rigaku X-ray generator was used for the WAXD experiments. The point focus beam was monochromatized to Cu Kα with a graphite crystal. X-ray powder diffraction data were recorded on a diffractometer. A temperature controller was added to the X-ray apparatus for thermal measurements. The precision of the controller was ±0.5 K in the temperature range studied. Nonisothermal experiments were carried out at a constant cooling rate of 5 K/min. Isothermal experiments were conducted by quickly transferring the molten sample to the preset sample temperature controller. The total time necessary to transfer the sample and collect the first X-ray scan was about 1 min. In both cases thermal X-ray experiments were carried out parallel to the DSC experiments.

Small-Angle X-ray Scattering (SAXS). Time-resolved SAXS measurements were conducted on the Oak Ridge National Laboratory beamline, X-14, at the National Synchrotron Light Source (NSLS).[24] The monochromator was tuned to 8.00 keV, which is equivalent to a wavelength of 1.5498 Å. A Mettler hot stage (FP-52) was mounted on a Huber goniometer with the position-sensitive proportional counter (PSPC) at a distance of 1.23 m. The shortest time for data collection was approximately 0.9 min. Lorentz correction of the SAXS data was applied by multiplying the intensity I (counts per second) with s^2 ($s = 2 \sin \theta/\lambda$, where λ is the wavelength of the synchrotron X-ray). The isothermal experiments on SAXS have the same procedure as in the DSC measurements.

Polarized Light Microscopy (PLM). A Nikon Labophotpol microscope with a 35-mm camera and a Mettler PF-52 hot stage were used for the optical microscopy experiments. Samples were prepared between two glass slides with a thickness of about 10 μm and held at 20 K above the melt temperature for 2 min. Nonisothermal experiments entailed cooling at 10 K/min to about 325 K. Isothermal experiments consisted of quickly transferring the molten sample to the preset temperatures in the hot stage and holding for various periods of time.

^{13}C Nuclear Magnetic Resonance Spectroscopy (NMR). The ^{13}C NMR measurements were carried out using a Nicolet NT200 spectrometer, operating at 200.07 and 50.31 MHz for ^{1}H and ^{13}C, respectively. A broad-band solid-state probe, purchased from Doty Scientific Inc., permitted variable-temperature measurements.

The ^{13}C NMR spectra of the isotropic melt were obtained using the method of one pulse with two-level decoupling of protons. The solid-state ^{13}C spectra were obtained using the methods of cross-polarization, high-power proton decoupling, and magic-angle sample spinning (CP-MAS). The dephasing experiments were carried out by inserting a dephasing delay, τ, ranging from 0 to 150 μs, between the spin locking/contact and decoupling of the proton spins in the CP-MAS pulse sequence (when $\tau = 0$ μs, this experiment is identical to the standard CP-MAS).[25] The samples were cooled from their isotropic melts at about 3 K/min.

Results

Transition Behavior in DSC Measurements. Figure 1 shows a set of DSC heating curves (heat capacity measurements) of MBPE-n samples, with n = 4–12, quenched from their isotropic melt to liquid nitrogen and immediately heated at 10 K/min. The glass transition temperatures, onset transition temperatures, and heats

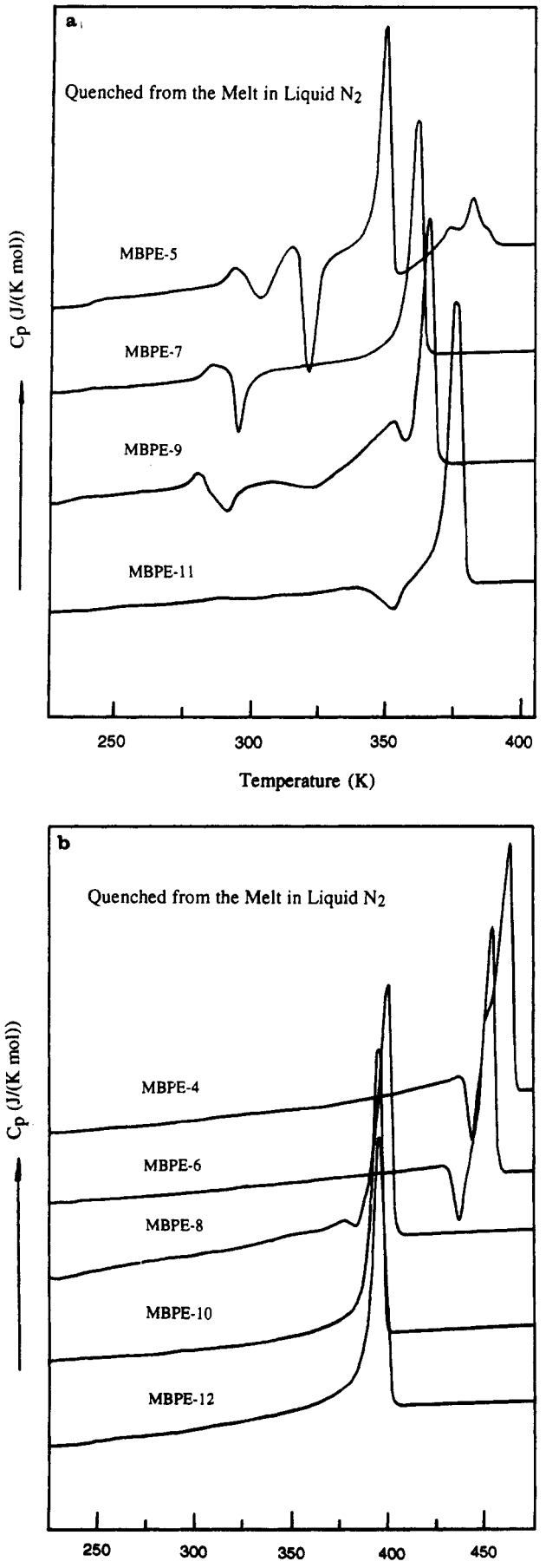

Figure 1. Heat capacities of MBPE-n (n = 4–12) polymers during heating after the samples were quenched from their isotropic melts to liquid nitrogen: (a) n = odd, (b) n = even.

Table II
MBPE-n Transition Temperatures and Heats of Transitions at a Heating Rate of 10 K/min[a]

n	T_g, K	T_{onset}, K	ΔH, kJ/mol
4	298.0	450.0	22.8
5	288.5	307.0[b]	-0.1
		342.0[b]	2.5[c]
		350.0[b]	-1.4[c]
		365.0[b]	5.2
6	291.0	441.0	21.4
7	279.6	352.3	10.4
8	261.0	387.0	19.9
9	272.0	355.5	18.2
10	269.4	385.1	31.1
11	277.0	365.2	20.6
12	272.2	382.4	28.4

[a] The samples were cooled to 220 K at 10 K/min before heating. [b] Approximate onset temperatures. [c] Transition overlap preceding and/or succeeding transition.

of transition observed at a heating rate of 10 K/min after cooling at 10 K/min are listed in Table II.

MBPE-5 is the only sample which may be quenched to its isotropic glass state. This polymer has a complicated phase transition behavior, and details of these transitions have been addressed in a previous publication.[26]

The heating curve of MBPE-7 exhibits an exothermic process immediately following the glass transition. The endothermic melting transition is larger in magnitude than this exotherm, and it is concluded that the sample is not quenched to the isotropic glass state. Efforts to reduce thermal gradients within the sample by decreasing the sample mass to 0.1 mg, and thereby increase the effective cooling rate on quenching, yielded results identical to those shown in Figure 1.

MBPE-9 and MBPE-11 and all of the polymers with an even number of methylene units could not be quenched to the isotropic glass states. As shown in Figure 1, no mesophase transition after melting can be observed for any of the polymers.

Nonisothermal experiments on the samples at different cooling rates are shown in parts a–d of Figure 2. The polymers with an odd number of methylene units in the flexible spacer (5, 7, 9, and 11) have at least two transitions on cooling and, depending on cooling rate, sometimes three (for MBPE-9 when the cooling rate is faster than 10 K/min). Note that at cooling rates of 10 K/min and slower MBPE-7 has only one transition and at rates of 20 K/min and faster two transitions become evident.

The first transition observed on cooling shows that the onset temperature and the heat of transition are independent of the cooling rate. The subsequent transitions decrease in both temperature and heat of transition with increasing cooling rate.

The polymers with an even number of methylene units in the flexible spacer show only one transition at all cooling rates studied. Interestingly, these transitions are cooling-rate independent as well. The magnitudes of these transitions are in the range of 20–46 kJ/mol. Table III lists the thermal transition properties on cooling for all MBPE polymers.

Isothermal experiments were conducted for the MBPE-n=odd polymers only. Isothermal temperatures were chosen both above and below the temperature at which the first peak is observed on cooling. Figure 3 shows two isothermal experiments of MBPE-9 at T_c = 345.4 and 343.6 K. At T_c = 345.4 K, a single exothermic peak with ΔH = 12.1 kJ/mol is observed. However, the same MBPE-9 sample below that temperature exhibits two distinct exothermic processes, the first having an enthalpy of

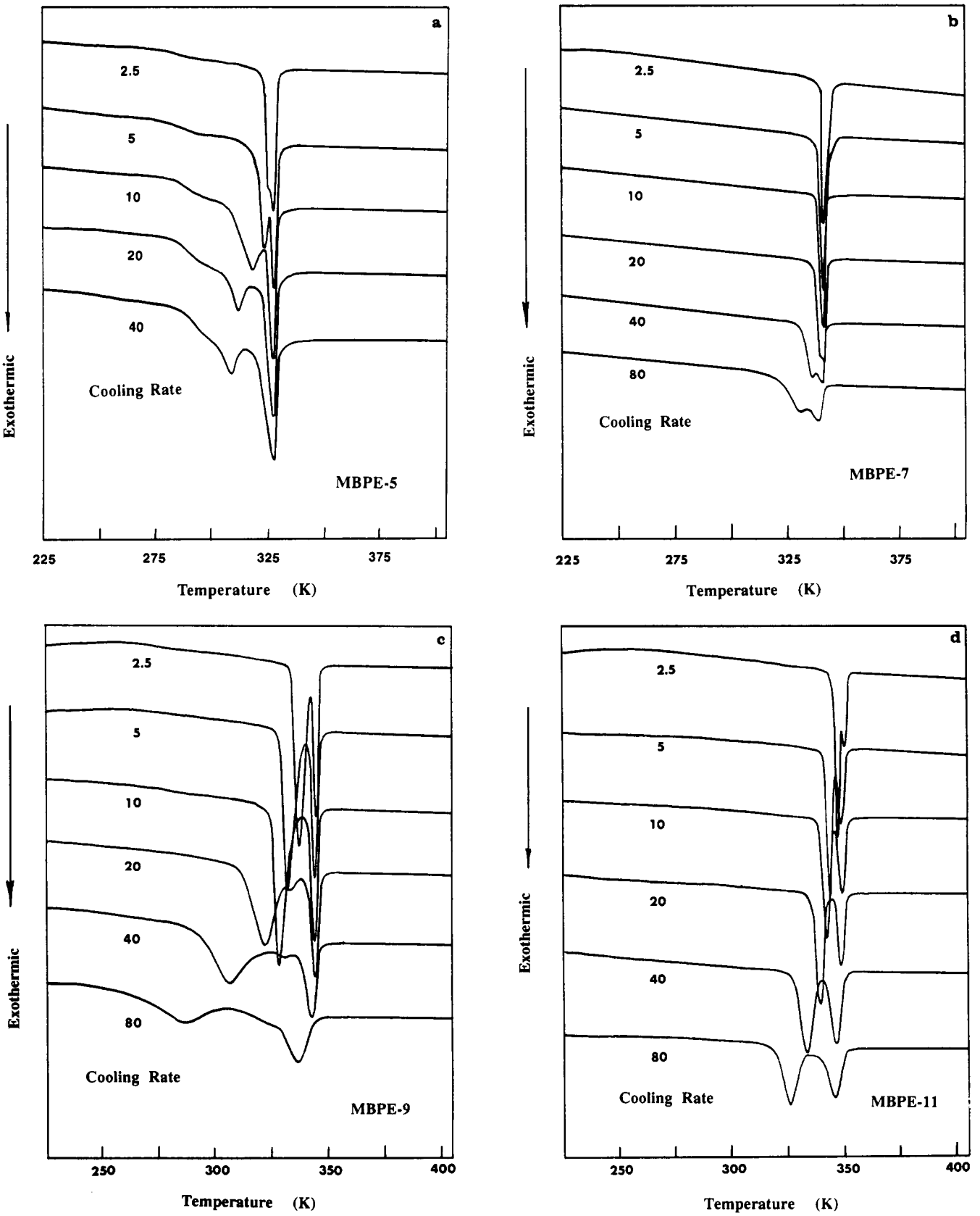

Figure 2. Nonisothermal DSC experiments at different cooling rates from the melt for (a) MBPE-5, (b) MBPE-7, (c) MBPE-9, and (d) MBPE-11.

transition nearly identical to the first peak observed on cooling of 5.40 kJ/mol (see Figure 2c). The second peak has an enthalpy of transition of 8.7 kJ/mol. A detailed analysis of the isothermal crystallization process will be addressed in a later publication.[27] The importance of this data for the present analysis is the observation of two exothermic processes when the polymers are crystallized below the temperatures at which the first peak is observed on cooling. Similar isothermal DSC data is observed for MBPE-5 below 330 K and MBPE-11 below 350 K. MBPE-7 shows only one peak during all isothermal crystallization experiments.

Table III
MBPE-*n* Temperatures and Heats of Transitions Cooling from the Isotropic Melt at 10 K/min

n	T_{onset}, K	ΔH, kJ/mol	*n*	T_{onset}, K	ΔH, kJ/mol
4	446.5	-23.4	9	345.6	-5.78
5	329.3	-3.00		331.0	-12.0
	318.0	-2.90	10	382.1	-28.9
6	439.1	-19.4	11	350.5	-6.70
7	343.7	-9.79		344.0	13.5
8	393.5	-17.4	12	374.8	-25.6

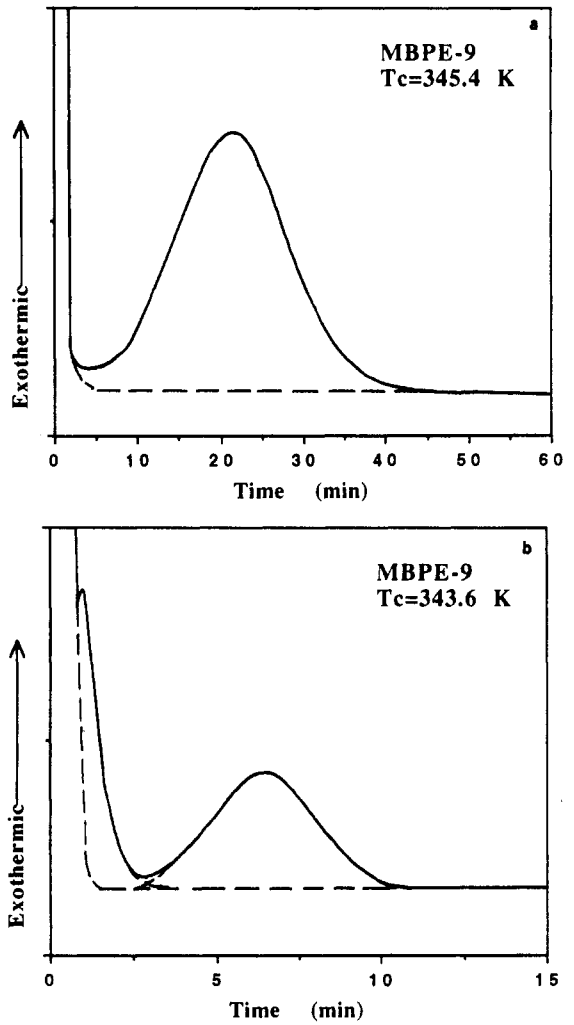

Figure 3. Isothermal DSC experiments for MBPE-9 crystallized at (a) 345.4 and (b) 343.6 K.

Sequential cooling and heating experiments on MBPE-9 are shown in Figure 4. The sample is cooled at 10 K/min to just below the end of the first transition (340 K). The onset temperature and the enthalpy of transition on cooling are 346 K and 5.60 kJ/mol, respectively. The sample is then reheated immediately (t_c = 0 s). The onset temperature and the enthalpy of transition on heating are identical to those values observed on cooling. A second, smaller, transition is observed with an onset temperature at about 356 K, which corresponds to the melting process in Figure 1. The sample is held for various times at 340 K for the subsequent experiments. As t_c increases, the first peak (346 K) decreases, while the higher temperature peak (356 K) increases. After about 6 min the process is complete and only the high-temperature peak remains. The magnitude of the enthalpy of the high-temperature transition has also surpassed that of the low-temperature peak to a final value of 15.9 kJ/mol.

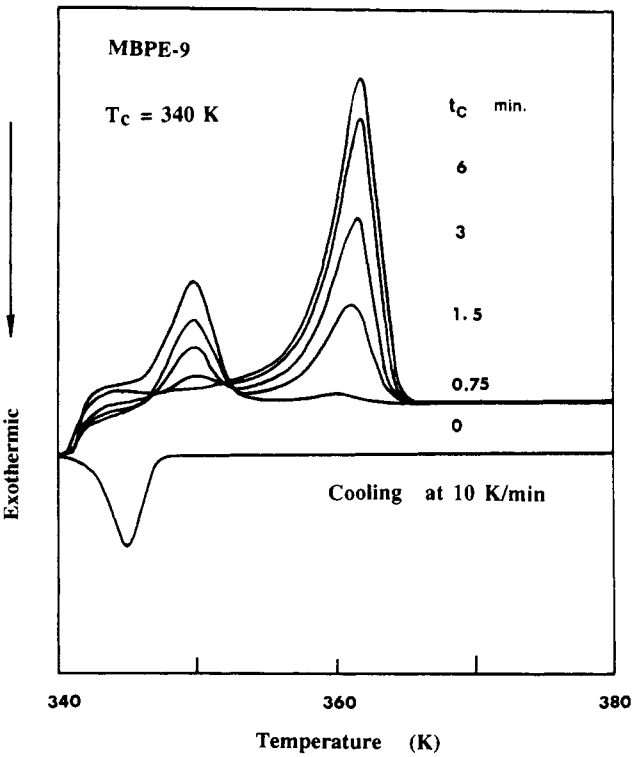

Figure 4. Set of DSC heating traces of MBPE-9 after the sample was cooled from its melt at 10 K/min and isothermally kept at 340 K for different times (0–6 min).

Structure Formation Observed through WAXD and SAXS Experiments. Nonisothermal WAXD experiments were only carried out for the polymers with an odd number of methylene units (n = 5, 7, 9, and 11). Figure 5 shows successive WAXD patterns during cooling at 5 K/min and the corresponding temperatures for MBPE-9, as an example. The samples exhibit an amorphous pattern above their respective melt temperatures. As the sample is cooled to the temperature of the first transition, the peak position shifts to higher 2θ values (lower d-spacing). However, despite the heats of transition detected from DSC, no diffraction peak is observed when the temperature passes through the first transition. On continued cooling, crystalline diffraction peaks develop at about the temperatures at which the second peak is observed in the DSC cooling measurements. For MBPE-5 and -11, similar observations can also be found. Figure 6 shows the d-spacing (calculated from Bragg's law) as a function of temperature; notice the sharp drop at about 330 K for MBPE-5, at 346 K for MBPE-9, and at 351 K for MBPE-11. This drop for MBPE-7 cannot be observed since two transition peaks can only be observed when the cooling rate is faster than 10 K/min (Figure 2b).

Isothermal WAXD experiments are carried out at temperatures slightly below the temperature at which the first transition is observed in the DSC cooling experiments. The diffraction data are initially structureless with average intermolecular spacings similar to those of amorphous samples. As the time increases, X-ray data remain structureless while the maximum in the peak shifts to a higher 2θ angle (lower d-spacing). Crystal diffraction peaks rapidly develop at longer time (on the order of 2–5 min). The exception is MBPE-7 which always exhibited crystalline diffraction peaks in the temperature range of interest. The data are listed in Table IV.

Figure 7 shows a set of time-resolved SAXS curves for MBPE-5 isothermally crystallized at 325.0 K, as an example. It is evident that, at the shortest isothermal

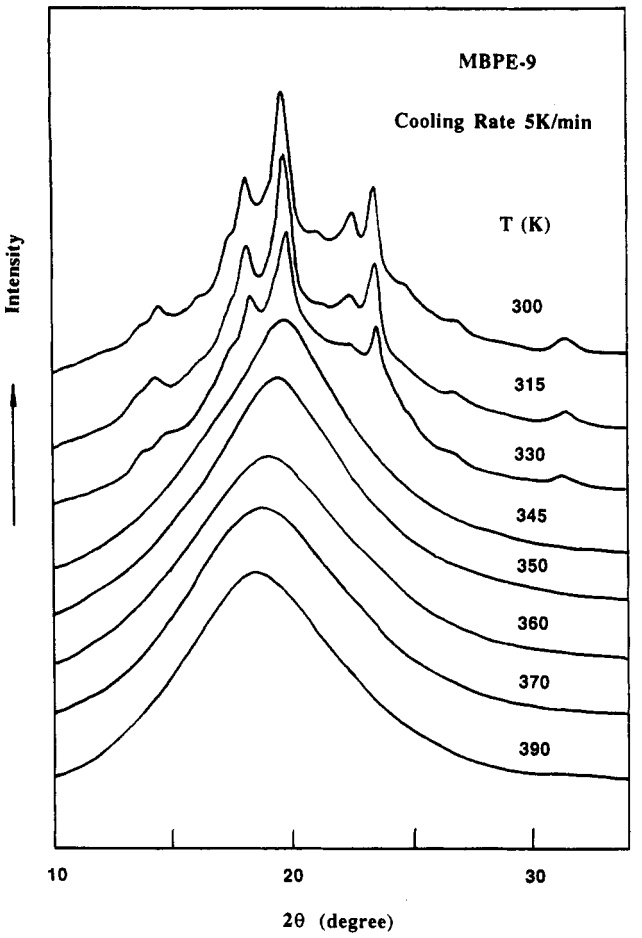

Figure 5. WAXD patterns during cooling at 5 K/min from the melt for MBPE-9.

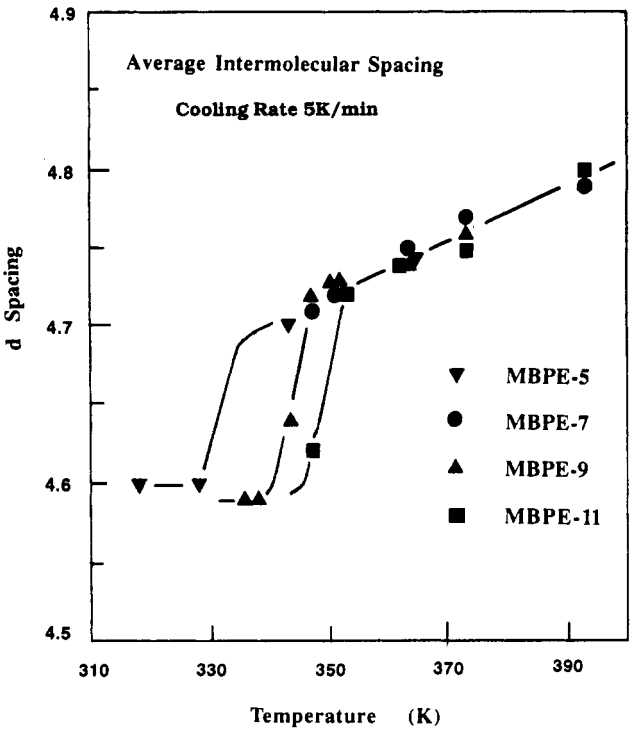

Figure 6. Relationships of the d-spacing of WAXD broad patterns before crystallization with temperatures.

time of 0.9 min, a long spacing of 29.0 nm can be observed. With an increase in the time to 2.3 min, the long spacing is slightly decreased to 27.5 nm. After times longer than

Table IV
d-Spacing Change of MBPE-n=odd during Isothermal WAXD Experiments

	t_c, min	2θ	d, Å
MBPE-5, T_c = 323 K			
	0.5	19.0	4.66
	1.3	19.3	4.59
MBPE-7, T_c = 338 K			
	0.5	crystalline diffraction peaks	
MBPE-9, T_c = 343 K			
	0.5	18.9	4.69
	1.3	19.2	4.62
MBPE-11, T_c = 348 K			
	0.5	18.9	4.69
	1.0	19.3	4.59

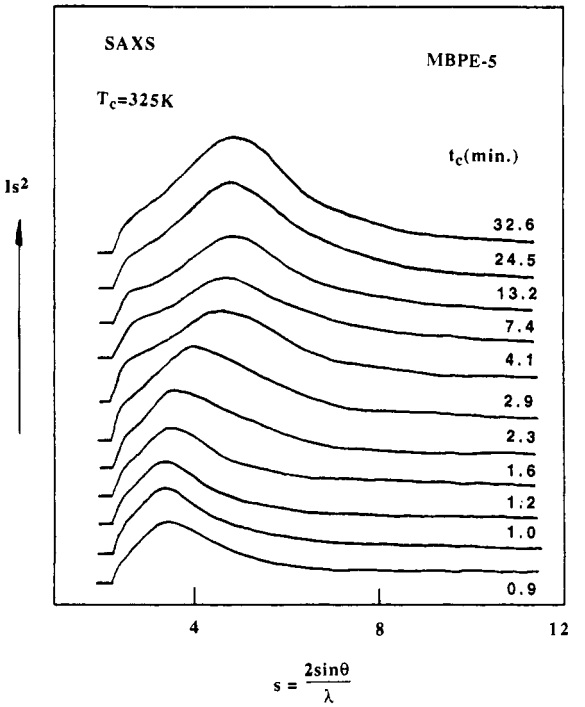

Figure 7. Set of time-resolved SAXS curves for MBPE-5 isothermally crystallized at 325.0 K.

2.3 min, the long spacing exhibits a further shift to a wider angle which corresponds to a spacing of 21.5 nm, and only a minor, continuous decrease of the long spacing can be seen at even longer crystallization times. For example, this long spacing is 21.0 nm after t_c = 32.6 min. Other MBPE-n=odd polyethers show a similar behavior in the SAXS measurements when the isothermal experiments are carried out at temperatures between two transitions during cooling (see Figure 2).

Morphological Changes in PLM Observations. All samples crystallized nonisothermally at a cooling rate of 10 K/min exhibit rapid phase transitions. The polymers with an odd number of methylene groups in the spacer (n = 5, 7, 9, and 11) become birefringent almost instantaneously (after about 5–10 s) at temperatures corresponding to the first peak observed on cooling in the parallel DSC measurements. The texture is very fine and "grainy", with less clear identification of disclination points or "threadlike" texture compared with the normal textures of the nematic liquid-crystal polymers. Polymers with an even number of methylenes (n = 4, 6, 8, 10, and 12) also exhibit rapid phase transitions on cooling. The temperatures at which these transitions occurred are the same as the single transition observed in the DSC measurements. The texture of the MBPE-n=even is qualitatively similar to that in the case of MBPE-n=odd described above.

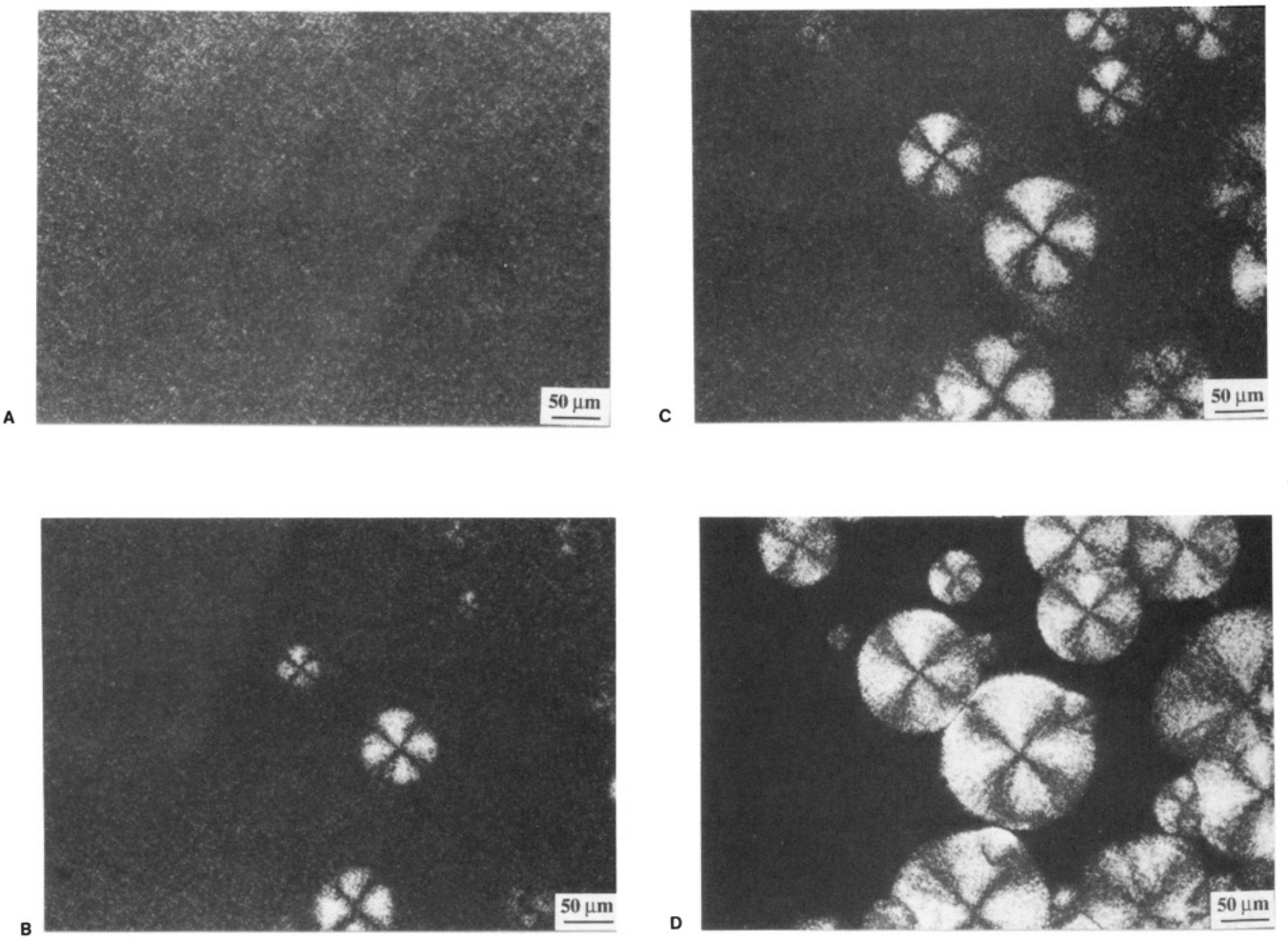

Figure 8. PLM observations of MBPE-11 crystallized at 348.2 K for (A) t_c = 0.5 min, (B) t_c = 5.0 min, (C) t_c = 10.0 min, (D) reheating to 352.2 K after C.

Isothermal experiments were conducted primarily on the MBPE-*n*=odd homologues. Samples were isothermally held above the temperatures at which the first transition is observed on cooling, resulting in crystallization from the isotropic melt. MBPE-5 exhibits several different crystalline morphologies depending on the crystallization temperature. The details of this crystallization have been addressed in a recent publication.[26] MBPE-7 grows many small crystallites at all the temperatures even above the first transition observed in the DSC cooling measurements; normal polymeric spherulites were not observed for this polymer. MBPE-9 and MBPE-11 grow typical spherulites at temperatures above 346 and 350 K, respectively. The crystal morphologies will be discussed in detail in a future publication.[27]

Samples isothermally held at temperatures below the first transition on cooling have a much different behavior. Each of the polymers with n = odd rapidly becomes birefringent in a manner similar to that described for the nonisothermal experiments. The MBPE-5 and MBPE-7 polymers crystallize very quickly and qualitatively retain the same fine, grainy texture. MBPE-9 and MBPE-11, however, rapidly become birefringent as before, but the growth of spherulites quickly ensues for both of these polymers. Immediate reheating after a short isothermal time results in the disappearance of the portion that was initially birefringent but the retainment of the spherulites which start growing during isothermal crystallization. A series of time-resolved pictures followed by reheating are shown in parts A–D of Figure 8 for MBPE-11, as an example. Similar observations have also been found in MBPE-9 samples with minor modifications.

^{13}C NMR Spectra at Variable Temperatures. The repeating unit of MBPE-9 is shown here with the numbering of the distinguishable carbon atoms used in this paper, as an example

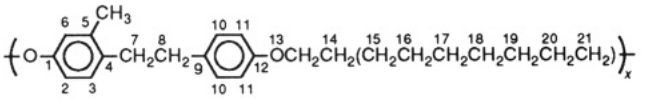

The chemical shift assignments for all the carbons are determined from the spectra of the melt (Figure 9A) based on the consideration of substituent effects.[28] The temperature dependence of the chemical shifts of all carbons in the CH_2 sequences will be presented and discussed elsewhere based upon the γ-gauche effect of conformational isomerism.[28] The ^{13}C spectra measured with CP-MAS and dephasing at 338 and 310 K, where two transition peaks are observed from the DSC cooling trace, are shown in parts B–E of Figure 9. The methyl carbon resonances are always intense, presumably because the rapid methyl group rotations reduce the ^{13}C–^{1}H dipolar coupling. It is evident that the signal intensities are suppressed with decreasing temperature. However, such suppressions are in different degrees. The sample is cooled through the transition at 345.6 to 338 K; the data are shown in parts B and C of Figure 9 at 338 K. The signal intensities of nonprotonated carbons C-1, C-4, C-5, C-9, and C-12 are the least affected when compared to those of protonated carbons, while the signals from the protonated aromatic

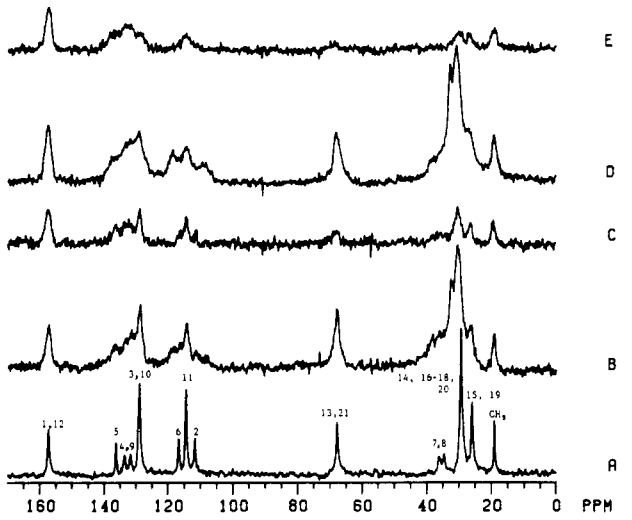

Figure 9. ^{13}C NMR spectra of MBPE-9 (A) in the isotropic melt, (B) at 338 K measured with CP-MAS, (C) at 338 K measured with dephasing (a delay of 70 μs), (D) at 310 K measured with CP-MAS, and (E) at 310 K measured with dephasing (a delay of 70 μs).

carbons, C-2, C-3, C-6, C-10, and C-11, have been moderately suppressed. The greatest signal suppression is, however, achieved on the central methylene carbons, C-15 to C-19. On the other hand, through the transition of 331.0 K (parts D and E of Figure 9 at 310 K), the signal intensities of C-2, C-3, and C-6 are completely suppressed, while the signals from the protonated carbons on the other phenylene ring (C-10 and C-11) are still present. The central methylenes (C-15 to C-19) continuously decrease their intensities but are less pronounced than those of the aromatic atoms. At the same time, the signals of C-13, C-14, C-20, and C-21 are also not fully eliminated.

Discussion

A combination of DSC, WAXD, SAXS, PLM, and solid-state NMR experiments proves that the polymers with an odd number of methylene units form a mesophase on cooling. Crystallization rapidly follows the mesophase transition in both nonisothermal and isothermal experiments. The mesophase transition is essentially cooling-rate independent with respect to the onset temperature of transition and the enthalpy of transition. This behavior is typical for liquid crystallinity. For other mesophases, we have also shown, for example, that polyoxybenzoate and its copolymers with oxynaphthoate freeze almost instantaneously to the hexagonal mesophase state and anneal only after further cooling or at much longer times to the orthorhombic crystal.[29] The melting temperature of the crystals is higher than the mesophase transition, and, therefore, the mesophase cannot be observed on heating the crystallized samples. This type of mesophase transition behavior has been termed monotropic. The particulars of the crystallization process will not be addressed at this time; rather the focus will be on the mesophase transitions only. Special attention has been paid to the MBPE-9's three transition phenomena during cooling when the cooling rate is faster than 10 K/min. The first two transitions have been characterized to be mesophases ("uniaxial nematic phases" in ref 30), and the last exothermic peak is attributed to the crystallization.[30]

The MBPE polymers with an even number of methylene units in the spacer have only one transition on cooling. The onset temperature of this transition and heat of transition are also very nearly cooling-rate independent (Table III). The enthalpy of transition is quite large, and the samples are solid after cooling from the melt. The conclusion is drawn that these materials crystallize on cooling. The conspicuous lack of a mesophase transition in any of the polymers with n = 4, 6, 8, 10, or 12 in combination with the cooling-rate-independent transition properties leads to the speculation of an experimentally unresolvable (and inaccessible) mesophase for these polymers. Another possibility may also exist for these polymers; namely, the polymers may crystallize from the melt sufficiently rapidly to preclude a separate mesophase transition. However, the general understanding of a crystallization process is that supercooling is cooling-rate dependent. This is contrary to the observations here studied.

Isothermal crystallization of the MBPE-n=odd samples is possible at temperatures both above and below the mesophase transition. However, the mesophase transition is difficult to bypass. At isothermal temperatures below this transition, crystals grow from the mesophase, while at temperatures above the transition crystallization takes place from the isotropic melt (Figures 3, 4, and 7 here and Figures 5–8 in ref 26).

Nonisothermal WAXD experiments support the assignment of a mesophase to the first transition observed on cooling. WAXD patterns of the molten samples display a sudden shift in the peak maximum to higher 2θ values (lower d-spacing) at temperatures corresponding to the first transition observed in the DSC cooling experiments (Figures 2 and 5). No diffraction peaks are detected immediately after this shift. Continued cooling of the samples resulted in the rapid development of crystalline diffraction peaks, except for the case of MBPE-7.

Nematic liquid crystals have wide-angle X-ray powder diffraction patterns similar to that of an amorphous halo. The average intermolecular distance as measured by the peak of the X-ray diffraction, however, is lower than that of the amorphous material.[31] This is the situation observed for the MBPE polymers with n = 5, 9, and 11. These data prove that the sample is nematiclike and eliminate the possibility of any higher order smectic liquid-crystalline phases.[32-34] Similar observations for MBPE-9 and other copolyethers have been reported recently by Ungar et al.[35]

Isothermal WAXD experiments were able to detect the rapid transition from the isotropic melt to the mesophase. The first WAXD scan at the temperature below the mesophase transition corresponds to the d-spacing of the polymer during the mesophase transition. The next scan, which has a maximum at higher 2θ angles, is after phase transition to the mesophase state.

Of special interest is the change of the long spacing between the mesophase state and the crystal state as observed from SAXS (Figure 7). One assumes that in this mesophase state only one-dimensional, orientational order is retained. The long spacing of 29.0 nm should thus be representative of the correlation length of the long-range orientational order, rather than two phases coexisting in this state. On the other hand, the long spacing of 21.5 nm formed during the crystallization is due to lamellar crystals. A quick shift (decrease) of the long spacing occurs in a short period of time (usually a few minutes). The orientationally ordered mesophase may also act as a precursor to further crystal growth.

Polarized light microscopy was employed in the identification of the monotropic mesophase. Samples cooled at 10 K/min remained amorphous until the temperatures correspond to the first transition observed in the DSC cooling experiments. The rapid development of birefrin-

gence at these temperatures is typical of a mesophase transition. Crystallization immediately follows the isotropic to mesophase transition, preventing the perfection of the mesophase texture over time.

Isothermal experiments conducted at temperatures below the mesophase transition lead to spherulitic growth from the mesophase state of MBPE-9 and MBPE-11 polymers. At intermediate crystallization times, the samples can be heated to destroy the mesophase of the material but retain the spherulites grown from this phase (Figure 8). Interestingly, the texture of the spherulites is different from the spherulitic texture grown directly from the isotropic melt at higher temperatures.[27] This shows that the crystal morphology is affected by the chain conformation and orientation of the initial state.

The ^{13}C NMR spectra have provided the most convincing evidence for molecular motion after both transitions during cooling. In the dipolar dephasing experiment, the decrease of the signal intensity as a function of the dephasing delay yields information on the values of effective spin–spin relaxation time (T_2) which depends strongly upon the mobility. On the basis of the different dephasing behaviors, the carbon atoms can be classified into three categories according to their number of attached protons and their mobility:[36] (1) Signals of rigid, protonated ^{13}C will be suppressed by virtue of dephasing because of their short spin–spin relaxation time (T_2) arising from strong and dispersed dipolar local fields. (2) Signals of mobile, protonated ^{13}C will be less suppressed because of their relatively long spin–spin relaxation time arising from partially averaged, therefore, weaker dipolar local fields. (3) Signals of nonprotonated ^{13}C will be the least affected because of an even longer spin–spin relaxation time resulting from the fact that they are far from any protons (>0.2 nm compared to 0.109 nm for a directly bonded C–H). From Figure 9, through the transition from the isotropic melt to the mesophase for MBPE-9, the greatest suppression of the signal intensities occurs on the central methylene carbons C-15 to C-19 among all the carbons in the repeating unit, indicating that the motion in this part is reduced most. This is consistent with the relatively large entropy contribution from the spacer as shown in Figure 10 (see below). This slow-down (but not stop) in motion may be due to orientational ordering. On the other hand, the ^{13}C NMR spectra of protonated aromatic carbons (C-2, C-3, C-6, C-10, and C-11) reveal a considerable remaining motion of the phenylene rings (presumably rotation about the 1,4-phenylene axis). This result can be associated with a rather small entropy contribution from the semiflexible mesogen in going from the melt to 338 K.

For the transition from the mesophase to the crystal, ^{13}C NMR spectra at 310 K show that the motion of the methyl-substituted phenylene ($C_6H_3CH_3$) is significantly reduced, but that of the other phenylene is still remaining. The difference in mobility between these two phenylene rings at 310 K is perhaps due to the strong steric interaction between the methyl and methylene (C-7) groups. This interaction is the intramolecular reason for hindering the ring rotation. The decrease of mobility of central methylene units (C-15 to C-19) is less pronounced than that of the aromatic region. Residual mobility of the terminal carbons C-13, C-14, C-20, and C-21 can also be seen. The motion at 310 K about the C–C bond exchange between trans and gauche conformations causes conformational disordering. Nevertheless, in order to keep orientational order, such an exchange must be a cooperative motion with its neighbors. A detailed discussion of the motion and disorder will be presented in ref 26, in which the temperature dependence of chemical shift values is analyzed based on the γ-gauche effect of conformational isomerism in the spacer. The results show that the number of C–C bonds that have changed conformation at transitions agrees with the entropy changes observed by DSC, and only certain types of conformational defects are possible, such as 2g1, 2g2, 2g3, and 3g3 kinks and jogs. Finally, it should be pointed out that the second mesophase in MBPE-9 during cooling has not been detected with NMR since the cooling rate of NMR measurements is too slow (~3 K/min).

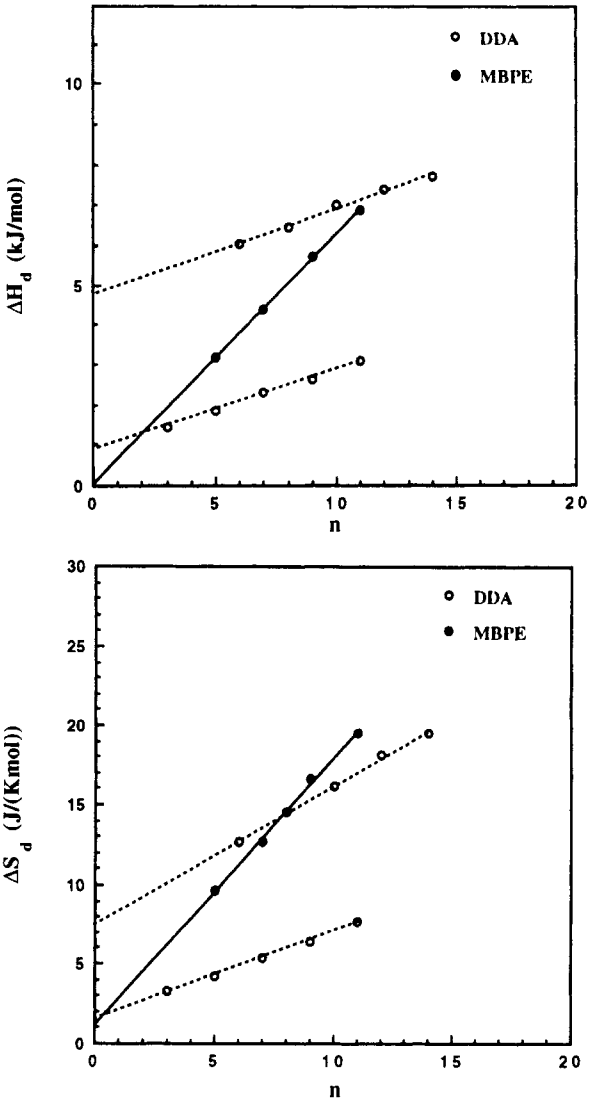

Figure 10. Relationship between the enthalpy of transition (ΔH_d) and the entropy of transition (ΔS_d) with the number of methylene units in the flexible spacer. The dashed lines are the data from ref 6 of ME9-Sn polymers.

It has been alluded to previously that the mesophase transition in this series of MBPE-n=odd polymers is near equilibrium in nature, identified by the independent transition temperature and the enthalpies of transition on cooling rate (see Figure 2). The enthalpy and the entropy of the mesophase transition are plotted against the number of methylene units in the flexible spacer in Figure 10. The magnitude of the enthalpy and the entropy of transition of the mesophase increases in a regular manner with increased numbers of methylene units in the flexible spacer. This phenomenon has also been observed for polymeric liquid crystals.[6,19] The increase has been attributed to the contribution from the flexible spacer (coupled to the mesogen) to the order in the liquid-

crystalline phase.[17,18] The mesogen contribution is often determined by extrapolating the data for ΔH_i and ΔS_i to a value of $n = 0$.[6]

The MBPE-n=odd polymers yield values very nearly $\Delta H_i = 0$ and $\Delta S_i = 0$ when extrapolated to $n = 0$. The slopes of the lines, however, are quite steep as shown in Figure 10 compared with liquid-crystalline polymers which are also included in this Figure.[6] The conclusion drawn from these data is that the semiflexible mesogenic portion of the polymers, although necessary for the formation of the mesophase, contributes little to the enthalpy and the entropy of transition. The experimental values are ΔH_i = 0.64 kJ/mol of methylene units and ΔS_i = 1.9 J/(K mol of methylene units). These data can be compared to those of Blumstein et al. for the enantiotropic liquid-crystalline ME9-Sn polymers which are based on the 2,2'-dimethylazoxybenzene mesogen with methylene flexible spacers[6] referred to in the Introduction. In the case of the MBPE-n=odd polymers, the enthalpy and the entropy of transition attributed to the flexible spacer are greater than those values assigned to the methylene units of the ME9-Sn polymers with both odd and even flexible spacers. It is thus shown that the flexible spacers in the MBPE polymers possess a higher degree of order in the mesophase than the corresponding methylenes in the ME9-Sn polymers. Finally, such kinds of contributions of the mesogens and flexible spacers for the liquid-crystal polyethers containing both rigid and semiflexible mesogens with methylene units have also been observed.[37]

Conclusions

MBPE polyethers have an experimentally accessible monotropic mesophase when the spacer contains 5, 7, 9, or 11 methylene units. Experimental evidence links the orientation within the mesophase primarily to the methylene units composing the flexible spacer coupled with the semiflexible mesogen. This conclusion leads to broadening of the normal view of mesophase formation where the mesogen is the portion of the molecule primarily oriented and a secondary contribution comes from the spacer and provides an extreme case that the flexible spacer is primarily attributed to the orientational order.

MBPE-n=even do not exhibit an experimentally accessible mesophase. A mesophase transition may also exist that is very rapidly followed by crystallization.

Acknowledgment. This work was partially supported by Exxon Education Foundation. S.Z.D.C. greatly acknowledges the support of his Presidential Young Investigator Award (DMR-9157738) from the National Science Foundation. This work was also supported in part by the Polymers Program of the National Science Foundation (DMR-8818412) at the University of Tennessee. Research was carried out (in part) from National Synchrotron Light Source (NSLS), Brookhaven National Laboratories, which is supported by the U.S. Department of Energy, Division of Materials Science and Division of Chemical Sciences. We also acknowledge the technical help of Drs. A. Habenschuss and P. R. Zschack for the SAXS experiments.

References and Notes

(1) Ruviello, A.; Sirigu, A. *J. Polym. Sci., Polym. Lett. Ed.* **1975**, *13*, 455; *Eur. Polym. J.* **1979**, *15*, 61; **1979**, *15*, 423; *Makromol. Chem.* **1982**, *183*, 895.
(2) Jackson, W. J., Jr.; Kuhfuss, H. J. *J. Polym. Sci., Polym. Chem. Ed.* **1976**, *14*, 2043.
(3) Menrisse, P.; Noel, C.; Monnerie, L.; Fayolle, B. *Br. Polym. J.* **1981**, *13*, 55.
(4) Griffin, A. C.; Havens, S. J. *J. Polym. Sci., Polym. Phys. Ed.* **1981**, *19*, 951.
(5) Anton, S.; Lenz, R. W.; Jin, J. I. *J. Polym. Sci., Polym. Chem. Ed.* **1981**, *19*, 1901.
(6) Blumstein, A.; Thomas, O. *Macromolecules* **1982**, *15*, 1264. Blumstein, R. B.; Stickles, E. M.; Blumstein, A. *Mol. Cryst. Liq. Cryst. (Lett.)* **1982**, *82*, 205.
(7) Blumstein, A.; Vilasagar, S.; Ponrathnam, S.; Clough, S. B.; Maret, G. *J. Polym. Sci., Polym. Phys. Ed.* **1982**, *20*, 877. Blumstein, R. B.; Stickles, E. M.; Gauthier, M.; Blumstein, A.; Volino, F. *Macromolecules* **1984**, *17*, 177.
(8) Krigbaum, W. R.; Astar, J.; Toriumi, H.; Ciferri, A.; Preston, J. *J. Polym. Sci., Polym. Lett. Ed.* **1982**, *20*, 109. Krigbaum, W. R.; Watanabe, J. *Polymer* **1983**, *24*, 1299.
(9) Lenz, R. W.; Jin, J. I. *Macromolecules* **1981**, *414*, 1405. Ober, C. K.; Jin, J. I.; Lenz, R. W. *Polym. J.* **1982**, *14*, 9. Lenz, R. W. *Faraday Discuss. Chem.* **1985**, *79*, 21.
(10) Sigaud, G.; Yoon, D. Y.; Griffin, A. C. *Macromolecules* **1983**, *16*, 875. Viney, C.; Yoon, D. Y.; Reck, B.; Ringsdorff, H. *Macromolecules* **1989**, *22*, 4088.
(11) Moore, J. S.; Stupp, S. I. *Macromolecules* **1987**, *20*, 273, 282; **1988**, *21*, 1222. Stupp, S. I.; Moore, J. S.; Martin, P. G. *Macromolecules* **1988**, *21*, 1228.
(12) Jonsson, H.; Werner, P.-E.; Gedde, U. W.; Hult, A. *Macromolecules* **1989**, *22*, 1683.
(13) Smyth, G.; Vallés, E. M.; Pollack, S. K.; Grebowicz, J.; Stenhouse, P. J.; Hsu, S. L.; MacKnight, W. J. *Macromolecules* **1990**, *23*, 3389.
(14) Laus, M.; Caretti, D.; Angeloni, A. S.; Galli, G.; Chiellini, E. *Macromolecules* **1991**, *24*, 1459.
(15) Cheng, S. Z. D.; Janimak, J. J.; Sridhar, K.; Harris, F. W. *Polymer* **1989**, *30*, 494; **1990**, *31*, 1122.
(16) de Gennes, P.-G. *Mol. Cryst. Liq. Cryst. (Lett.)* **1984**, *102*, 95.
(17) Abe, A. *Macromolecules* **1984**, *17*, 2280.
(18) Yoon, D. Y.; Bruckner, S. *Macromolecules* **1985**, *18*, 651.
(19) Blumstein, R. B.; Blumstein, A. *Mol. Cryst. Liq. Cryst.* **1988**, *165*, 361.
(20) Aharoni, S. M. *Macromolecules* **1988**, *21*, 1941. Aharoni, S. M.; Correale, S. T.; Hammond, W. B.; Hatfield, G. R.; Murthy, N. S. *Macromolecules* **1989**, *22*, 1137. Aharoni, S. M. *Macromolecules* **1989**, *22*, 686, 1125.
(21) Percec, V.; Tsuda, Y. *Macromolecules* **1990**, *23*, 3509.
(22) Percec, V.; Yourd, R. *Macromolecules* **1989**, *22*, 524.
(23) Percec, V.; Yourd, R. *Macromolecules* **1989**, *22*, 3229.
(24) Habenschuss, A.; Ice, G. E.; Sparks, C. J.; Neiser, R. A., Jr. *Nucl. Instrum. Methods* **1988**, *A266*, 215.
(25) Opella, S. J.; Frey, M. H. *J. Am. Chem. Soc.* **1979**, *101*, 5854.
(26) Cheng, S. Z. D.; Yandrasits, M. A.; Percec, V. *Polymer* **1991**, *32*, 1284.
(27) Yandrasits, M. A.; Cheng, S. Z. D.; Percec, V., in preparation.
(28) Cheng, J.; Jin, Y.; Wunderlich, B.; Cheng, S. Z. D.; Yandrasits, M. A.; Percec, V., in preparation.
(29) Cheng, S. Z. D. *Macromolecules* **1988**, *21*, 2475. Cheng, S. Z. D.; Janimak, J. J.; Zhang, A.-Q.; Zhou, Z.-L. *Macromolecules* **1989**, *22*, 4240.
(30) Ungar, G.; Percec, V.; Zuber, M. *Macromolecules* **1992**, *25*, 75.
(31) de Vries, A. *Mol. Cryst. Liq. Cryst.* **1970**, *10*, 219. See also: Wendorff, J. H. In *Liquid Crystalline Order in Polymers*; Blumstein, A., Ed.; Academic Press: New York, 1978; Chapter 1.
(32) Chandrasekhar, S. *Liquid Crystals*; Cambridge University Press: London, 1977.
(33) Helfich, W. *J. Phys., Colloq.* **1979**, *40*, 3.
(34) Pershan, P. S. *Structure of Liquid Crystal Phases*; World Scientific: Singapore, 1988.
(35) Ungar, G.; Feijoo, J. L.; Keller, A.; Yourd, R.; Percec, V. *Macromolecules* **1990**, *23*, 3411.
(36) Alla, M.; Lippmaa, E. *Chem. Phys. Lett.* **1976**, *37*, 260.
(37) Percec, V.; Kawasumi, M. *Macromolecules* **1991**, *24*, 6318.

Registry No. MBPE-4 (copolymer), 126366-74-3; MBPE-4 (SRU), 139407-77-5; MBPE-5 (copolymer), 115529-45-8; MBPE-5 (SRU), 139407-78-6; MBPE-6 (copolymer), 126366-71-0; MBPE-6 (SRU), 139407-79-7; MBPE-7 (copolymer), 115529-46-9; MBPE-7 (SRU), 139407-80-0; MBPE-8 (copolymer), 125370-76-5; MBPE-8 (SRU), 139407-81-1; MBPE-9 (copolymer), 115529-47-0; MBPE-9 (SRU), 139407-82-2; MBPE-10 (copolymer), 125370-77-6; MBPE-10 (SRU), 139407-83-3; MBPE-11 (copolymer), 115529-48-1; MBPE-11 (SRU), 139407-84-4; MBPE-12 (copolymer), 126419-34-9; MBPE-12 (SRU), 139407-85-5.